Effect of radiation-induced color centers absorption in optical fibers on fiber optic gyroscope for space application*

Jing Jin(金靖), Ya Li(李亚)†, Zu-Chen Zhang(张祖琛),
Chun-Xiao Wu(吴春晓), and Ning-Fang Song(宋凝芳)

School of Instrument Science and Optic-electronics Engineering, Beihang University, Beijing 100191, *China*

(Received 21 February 2016; revised manuscript received 4 April 2016; published online 25 June 2016)

The effects of color centers' absorption on fibers and interferometric fiber optical gyroscopes (IFOGs) are studied in the paper. The irradiation induced attenuation (RIA) spectra of three types of polarization-maintaining fibers (PMFs), i.e., P-doped, Ge-doped, and pure silica, irradiated at 100 Gy and 1000 Gy are measured in a wavelength range from 1100 nm to 1600 nm and decomposed according to the Gaussian model. The relationship of the color centers absorption intensity with radiation dose is investigated based on a power model. Furthermore, the effects of all color centers' absorption on RIA and mean wavelength shifts (MWS) at 1300 nm and 1550 nm are discussed respectively. Finally, the random walk coefficient (RWC) degradation induced from RIA and the scale factor error induced by MWS of the IFOG are simulated and tested at a wavelength of 1300 nm. This research will contribute to the applications of the fibers in radiation environments.

Keywords: color centers' absorption, radiation-induced attenuation, mean wavelength shift, fiber optical gyroscope

PACS: 42.81.Pa, 42.88.+h, 61.72.jn **DOI:** 10.1088/1674-1056/25/8/084213

1. Introduction

The interferometric fiber optical gyroscope (IFOG) is one of the most important achievements in the optical fiber sensing field, which can be used to measure vector rotation angular velocity relative to the inertial space and has been widely applied to spacecraft systems recently.[1,2] The sensing coil wound by optical fibers is the essential component of IFOGs. However, the presence of highly energetic radiation in space induces additional optical attenuation greatly. The radiation-induced attenuation (RIA) is primarily caused by the trapping of radiolytic electrons and holes at defect sites in the fiber.[3,4] Furthermore, it affects the performance of the IFOGs in space environment.[5] The smaller optical power received by the photodetector resulting from the RIA can cause the degradation of random walk coefficient (RWC). In Ref. [6], authors reported that the filtering effect arising from the wavelength-dependent RIA in the fiber coil can cause a change in the scale factor of an IFOG, but no experimental results exist. In Ref. [7], the change of wavelength centroid with time for a fiber coil during proton irradiation was tested, which showed a steady shift in wavelength. Moreover, the effect of the RIA spectrum dependence on the mean wavelength shift (MWS) during the light transmission can lead to the scale factor error.[8] It has been found that the RIA spectrum can be fitted by several color centers' absorption bands based on a Gaussian model.[9–11] A series of color centers have been studied in detail through special spectroscopic techniques.[12,13] Giacomazzi *et al.* presented a first-principles investigation of Ge paramagnetic centers in Ge-doped vitreous silica based on calculations of the electron paramagnetic resonance (EPR) parameters.[14] However, there are also some near-infrared (NIR) defects that are not so well-known, except for P-doped fibers, in which an NIR γ-induced absorption has already been attributed to P1 defects.[12] The RIA of fibers and its induced degradation on IFOGs have been investigated.[15] However, the correlation between the color centers' absorption and its influence on IFOGs are rarely studied. In addition, the effects of the radiation dose on the RIA and MWS of all color centers have not been studied, which will be helpful in assessing the performance of the space-borne IFOGs.

In this paper, to investigate the experimental spectrum results ranging from 1100 nm to 1600 nm in phosphorus (P)-doped, germanium (Ge)-doped, and pure-silica-core (PSC) PMFs at two radiation dose levels of 100 Gy and 1000 Gy, the Gaussian model is adopted based on the color centers' absorption. In addition, the influences of all color centers on RIA and MWS of the experimental fibers are discussed at the wavelengths of 1300 nm and 1550 nm respectively. Moreover, the relationship of the color centers' absorption intensity with radiation dose is investigated based on a power law model. Finally, the degradation of the RWC and the scale factor error of the IFOG induced by color centers' absorption are estimated and tested. The work will help to evaluate the performances of optical fibers and optical sensors in other radiation environments, such as military facilities and nuclear power plants.

*Project supported by the Scientific Research Foundation for the Returned Overseas Chinese Scholars, State Education Ministry, China.
†Corresponding author. E-mail: liyachinese@126.com
© 2016 Chinese Physical Society and IOP Publishing Ltd

2. Experimental setup

Three prototype PMFs with different dopants were chosen and irradiated by a ^{60}Co gamma radiation source at room temperature. Table 1 lists their main characteristics. The operating wavelength and cut-off wavelength of all fibers are 1300 nm and about 1100 nm. Fibers F1, F2, and F3 (F4, F5, and F6) were employed to compare for the discrepancy among different dopants of fibers, and the fibers F1 and F4 (F2 and F5 or F3 and F6) were used to analyze the effect of radiation dose on the RIA spectrum.

Table 1. Main characteristics of the fibers.

Fiber	Dopant	Length/km	Dose/Gy
F1/ F4	P∼1 mol%	0.3	100/1000
F2/F5	Ge∼15 mol%	0.3	100/1000
F3/F6	PSC∼none	0.3	100/1000

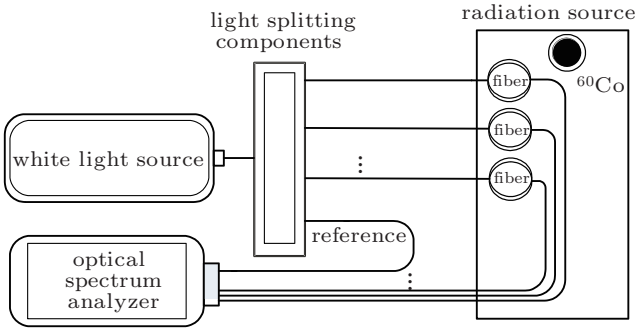


Fig. 1. Schematic diagram of the experimental setup.

The setup for measuring the RIA spectrum is shown in Fig. 1. A super continuum white light source with a spectrum width from 400 nm to 1700 nm was used, and its output signal was split into nine paths by light splitting components. Three were used as references to compensate for the variation of light intensity, and the others were used as interrogation signals. The RIA spectra of six experimental fibers were measured with an optical spectrum analyzer (OSA). The light source, the light splitters and the OSA were located outside the radiation room to avoid the influence of irradiation. The spectrum measurements were conducted in a wavelength range from 1100 nm to 1600 nm. Then the experimental fibers were annealed at room temperature for a few weeks until most of the unstable color centers had been decomposed and transformed after irradiation. The RIA spectrum can be obtained by using the following formula:

$$\mathrm{RIA}(\lambda) = L_{\mathrm{B}}(\lambda) - L_{\mathrm{A}}(\lambda), \tag{1}$$

where $\mathrm{RIA}(\lambda)$ represents the RIA spectrum, $L_{\mathrm{B}}(\lambda)$ the spectrum measured before irradiation, and $L_{\mathrm{A}}(\lambda)$ the spectrum measured after irradiation and annealing. The losses caused by coupling and instruments can be ignored, since their value is orders of magnitude smaller than that of the RIA.

3. Decomposition of the RIA spectra based on color centers' absorption

Since the types of color centers are directly related to the dopants in fibers, the radiation effects will depend on the composition of the fibers, such as core and cladding dopants, impurity levels, and stoichiometry.[16,17] However, these intrinsic parameters of the fibers are generally unavailable for the researchers who apply them to radiation study as these parameters are mostly considered to be confidential by the fiber manufacturers. Therefore, all common dopants are employed in this paper.

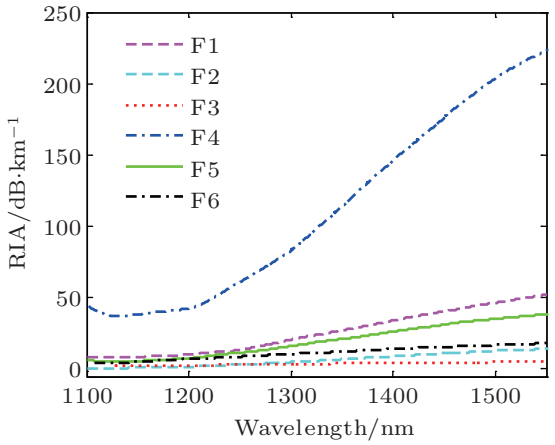


Fig. 2. (color online) Smoothed RIA spectra of six fibers.

Figure 2 shows the RIA spectra obtained from the experiments. The RIA spectra are smoothed appropriately. The RIA spectrum decomposition is to be addressed as the superposition of several corresponding color centers. Therefore, the RIA spectra are fitted by Gaussian functions[18] as widely assumed for defects in fibers. The fitting formula is expressed as

$$\mathrm{RIA} = \sum_{i=1}^{n} a_{\mathrm{i}} \exp\left[-\left(\frac{E - E_{\mathrm{i}}}{\omega_{\mathrm{i}}}\right)^2\right], \tag{2}$$

where E_{i} and ω_{i} represent the peak position and full width at half maximum respectively, E represents the photon energy, a_{i} the color centers' absorption intensity, and n the type of color centers. According to previous investigations, the values of E_{i} and ω_{i} of these color centers obtained at room temperature are listed in Table 2.[13,19,20]

Table 2. Main parameters values of color centers.

Center name	E_{i}/eV	ω_{i}/eV
PSC-STH	0.7	0.3
Ge-STH	0.72	0.3±0.1
P1	0.765	0.22
Ge-NBOHC	1.97	0.3–0.6
Si-NBOHC	2.0	0.18
Ge(X)	2.61	0.82

Substituting the values listed in Table 2 into Eq. (2), the fitting curves of RIA spectra can be obtained. The values of parameters may have subtle changes when fitting the data with higher precision. By the superposition of Gaussian functions, the RIA spectra can be decomposed. Figures 3(a)–3(f) illustrate the experimental smoothed spectra and decomposed results of six fibers. The corresponding color centers are also given there. The unit of horizontal axis in Fig. 3 is converted from nanometer (nm) to electron volt (eV).

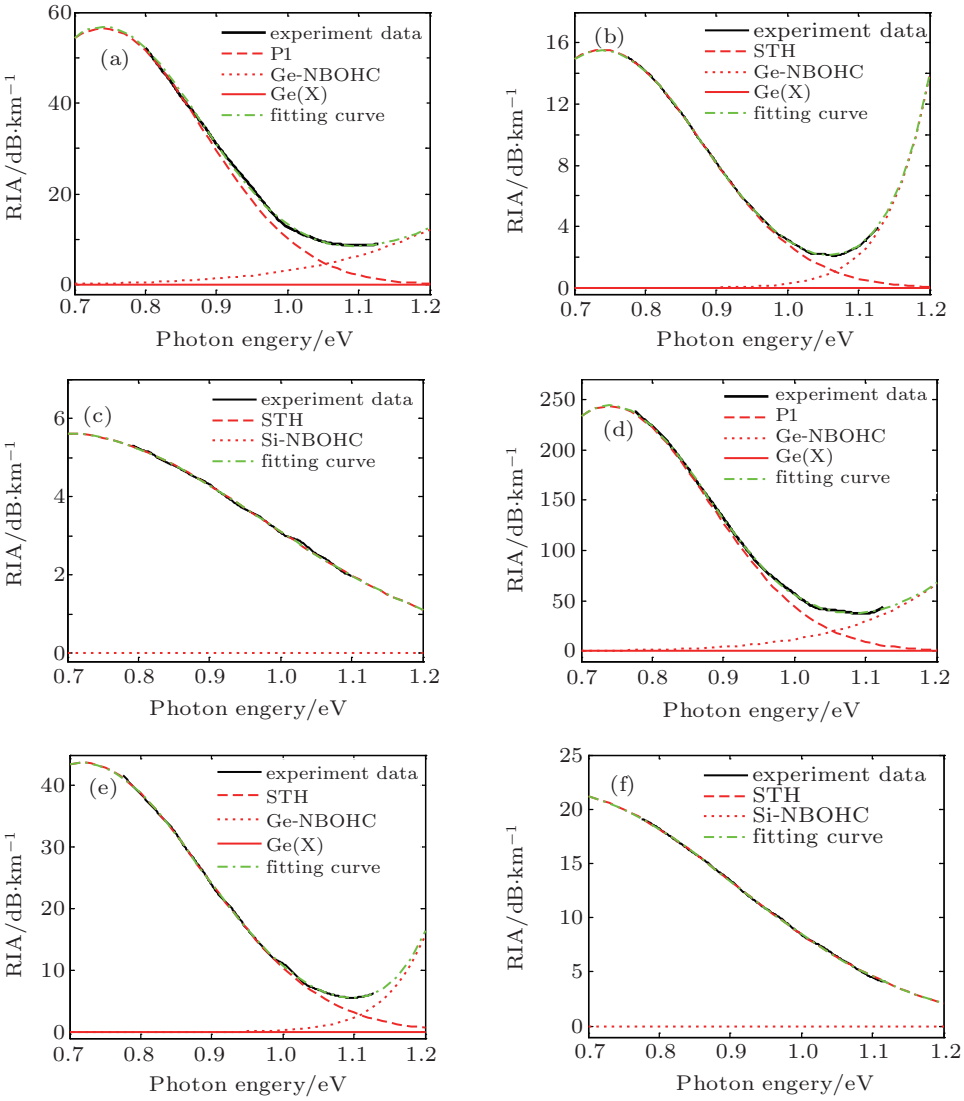


Fig. 3. (color online) RIA spectra and their fitting curves: (a) F1, (b) F4, (c) F2, (d) F5, (e) F3, (f) F6.

The RIA spectra result from three main contributions: the UV absorption tail, visible absorption bands, and NIR-contribution.[13] At the observation wavelengths, NIR absorption bands play the most important roles. The fitting results indicate that the RIA spectra of P-doped fibers can be decomposed into a sum of Gaussian functions corresponding to P1, Ge-NBOHC and Ge(X) color centers. The RIA spectra of Ge-doped fibers depend strongly on Ge-impacted Self-Trapped-Hole (STH) defects, Ge-NBOHC, and Ge(X) color centers. The RIA spectra of PSC fibers are decomposed by STH defects and the Si–NBOHC color centers. The fitting parameter values of the color centers are listed in Table 3. Thus the numerical fitting functions of fibers are obtained by inserting these values into Eq. (2).

Table 3(a). Parameter values of P-doped fiber.

Color center	Dose/Gy	a_i	E_i/eV	ω_i/eV
P1	100	56.44	0.74	0.199
	1000	243.1	0.74	0.199
Ge-NBOHC	100	162.8	1.962	0.5022
	1000	1447	2	0.456
Ge(X)	100	0.0005	2.618	0.756
	1000	0.001	2.621	0.763

Table 3(b). Parameter values of Ge-doped fiber.

Color center	Dose/Gy	a_i	E_i/eV	ω_i/eV
Ge-STH	100	15.53	0.7392	0.2003
	1000	43.76	0.7176	0.236
Ge-NBOHC	100	15450	1.994	0.3
	1000	19380	2	0.3
Ge(X)	100	0.0076	2.64	0.73
	1000	0.06944	2.64	0.7317

Table 3(c). Parameter values of PSC fiber.

Color center	Dose/Gy	a_i	E_i/eV	ω_i/eV
PSC-STH	100	5.622	0.692	0.4
	1000	21.59	0.65	0.3617
Si-NBOHC	100	4.59	2	0.18
	1000	18.39	2	0.18

4. Results and discussion

4.1. Effects of color centers' absorption on the fiber RIA and MWS

Each kind of color center has specific absorption characteristics, and it can absorb light in a specific wavelength range. Thus the wavelength dependence of the color centers' absorption may change the transmission properties of PMFs. The scale factor of IFOGs is associated with the mean wavelength of light signals, so it is necessary to study the characteristics of the MWS.

The mean wavelength λ can be calculated by the centroid of the spectrum weighted, which can be approximated by a linear weighting factor as follows:

$$\lambda = \frac{\sum_{i=1}^{n} P(\lambda_i)\lambda_i}{\sum_{i=1}^{n} P(\lambda_i)}, \tag{3}$$

where the sample spacing in the spectrum scan is 0.1 nm, $P(\lambda_i)$ is the optical power at the wavelength λ_i. To eliminate the influence of the MWS of the light source, the MWS of the RIA spectrum is corrected by the reference signal. According to Eq. (3) and Gaussian spectrum decomposition shown in Fig. 3, the RIA and the MWS of all color centers both at 1300 nm and 1550 nm under the same spectral width of 40 nm are calculated. The results at total doses of 100 Gy and 1000 Gy are listed in Tables 4 and 5, respectively.

Table 4. RIA and MWS computed at total dose of 100 Gy.

Fibers		RIA/(dB/km)		MWS	
		1300 nm	1550 nm	1300 nm	1550 nm
F1	P1	17.786	51.536	–1.355	–0.781
	Ge-NBOHC	2.894	0.581	0.0124	0.027
	Ge(X)	3.658×10^{-6}	1.433×10^{-6}	0	0
F2	Ge-STH	4.925	14.163	–0.373	–0.214
	Ge-NBOHC	0.093	0.002	0.015	0.0003
	Ge(X)	3.663×10^{-5}	1.32×10^{-5}	0	0
F3	PSC-STH	3.663	5.227	–0.085	–0.035
	Si-NBOHC	9.813×10^{-15}	2.290×10^{-19}	0	0

Table 5. RIA and MWS computed at total dose of 1000 Gy.

Fibers		RIA(dB/km)		MWS	
		1300 nm	1550 nm	1300 nm	1550 nm
F4	P1	76.608	221.975	–5.5571	–3.33925
	Ge-NBOHC	7.493	1.422	0.53545	0.08208
	Ge(X)	4.819×10^{-6}	1.741×10^{-6}	0	0
F5	Ge-STH	16.065	38.738	–0.964	–0.57251
	Ge-NBOHC	0.101	0.002	0.017	0.0003
	Ge(X)	0.0003	0.0001	0.00002	0.000004
F6	PSC-STH	10.661	18.179	–0.351	–0.208
	Si-NBOHC	3.932×10^{-14}	9.175×10^{-14}	0	0

As illustrated in Tables 4 and 5, the RIA and MWS of all color centers dramatically increase with increasing the radiation dose both at 1300 nm and 1550 nm for all fibers. It can be concluded that the proportion of the P1 color centers' absorption is more than 80% of the total RIA both at 1310 nm and 1550 nm, which are in agreement with those of the P1 color centers with an absorption peak around 1600 nm in P-doped fiber that the P1 fiber color centers' absorption is the main origin of the RIA at NIR waveband. For F5 and F6, almost all the total RIA is ascribed to the STH band. In addition, the RIA and MWS of all fibers at 1550 nm are more sensitive to radiation than at 1300 nm. Therefore, the 1300 nm is the better operational wavelength than 1550 nm for space IFOGs.

The RIA can be explained with the power-law model

$$A = CD^f, \tag{4}$$

where A is the RIA, D is the total radiation dose, and C and f are experimental constants. This model is capable of predicting or fitting the radiation responses of different fibers in a wide range with various degrees of accuracy.[21,22] Provided the color centers in the fiber remain stable, and the E_i and ω_i are not influenced by radiation dose in theory, the RIA spectrum as well as the color centers at any dose, not only 100 Gy

and 1000 Gy, can be fitted by combining power-law fitting functions and Eq. (2). Furthermore, the RIA values of different operating wavelengths at any dose can be obtained by

$$\begin{aligned}\mathrm{RIA}(E,D) &= \sum_{\mathrm{i}=1}^{n}\mathrm{RIA}_{\mathrm{i}}(E,D)\\ &= \sum_{\mathrm{i}=1}^{n} a_{\mathrm{i}}(D)\exp\left[-\left(\frac{E-E_{\mathrm{i}}}{w_{\mathrm{i}}}\right)^2\right],\end{aligned} \tag{5}$$

which can be considered as the model for the sensitivity of RIA spectra to dose.

The relationship between the color centers' absorption intensity and the radiation dose is studied quantitatively. It can be concluded that the color centers' absorption intensity and radiation dose conform to the power law relationship. The fitting curves are shown in Fig. 4. Table 6 gives the coefficients of the fitting function and their R^2. R^2 representing the degree of curve fitting is close to 1, and the fitting effect is better.

Table 6. Coefficients of fitting functions of $a_{\mathrm{i}}(D)$.

Fitting function: $a_{\mathrm{i}}(D) = C * D^f$				
Fibers	$a_{\mathrm{i}}(D)$	C	f	R^2
P-doped	P1	3.042	0.6342	1
	Ge-NBOHC	2.061	0.9488	1
	Ge(X)	0.0001182	0.3109	0.9996
Ge-doped	Ge-STH	1.956	0.4499	1
	Ge-NBOHC	9819	0.09843	1
	Ge(X)	9.104×10^{-5}	0.9608	1
PSC	PSC-STH	0.3812	0.5844	1
	Si-NBOHC	0.2859	0.6028	1

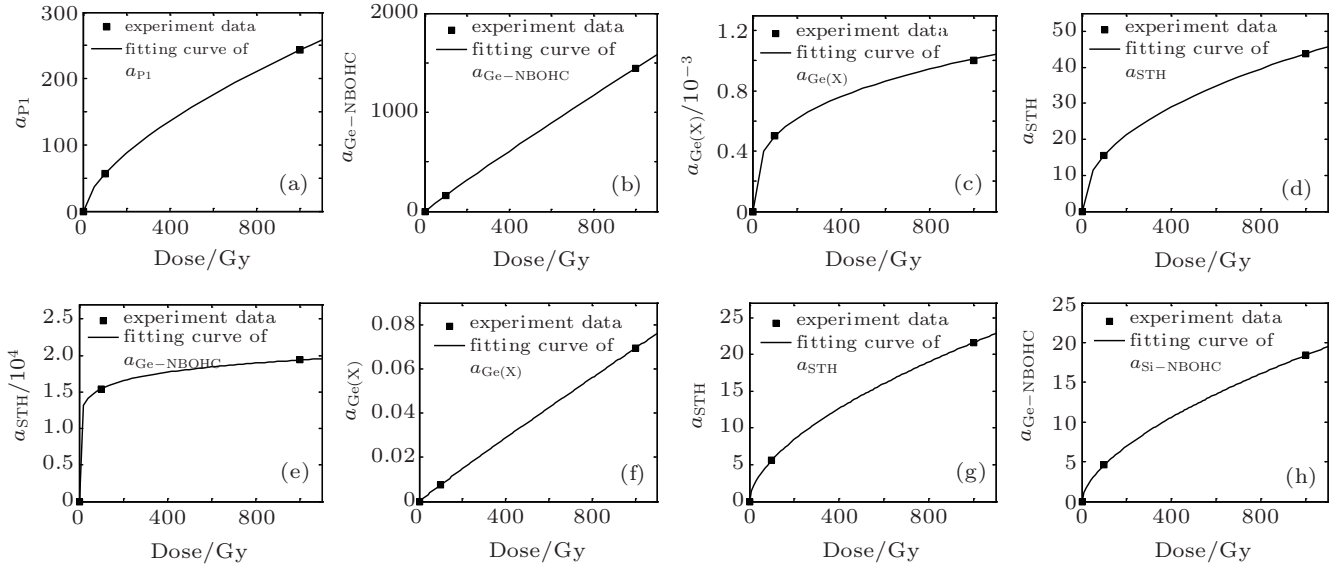


Fig. 4. Fitting curves of a_{i} versus dose: (a) a_{P1} (P-doped), (b) $a_{\mathrm{Ge-NBOHC}}$ (P-doped), (c) $a_{\mathrm{Ge(X)}}$ (P-doped), (d) $a_{\mathrm{Ge-STH}}$ (Ge-doped), (e) $a_{\mathrm{Ge-NBOHC}}$ (Ge -doped), (f) $a_{\mathrm{Ge(X)}}$ (Ge -doped), (g) $a_{\mathrm{PSC-STH}}$ (PSC), (h) $a_{\mathrm{Si-NBOHC}}$ (PSC).

4.2. Effect of color centers' absorption on the IFOGs

The scale factor error ε_{k} of IFOGs caused by the MWS can be computed from the following formula:[23]

$$\varepsilon_{\mathrm{k}} = \frac{\Delta\lambda}{\lambda}\frac{2\pi LD}{\lambda c}, \tag{6}$$

where L and D are the length and average diameter of the fiber coil, λ and $\Delta\lambda$ represent the mean wavelength and its variation respectively, and c is the speed of light. Moreover, RWC is an important parameter of optical fiber gyro static index, which determines the minimum of the gyro testing phase shift. The RWC of the closed-loop operational IFOG with $\pi/2$ modulation phase can be expressed as[5]

$$\mathrm{RWC} = \frac{\lambda c}{2\pi LD} \times\sqrt{\frac{2e}{\eta P10^{-(A_{\mathrm{C}}+AL)/10}}+\frac{1}{\Delta\nu}+\frac{4k_{\mathrm{B}}T}{R[\eta P10^{-(A_{\mathrm{C}}+AL)/10}]^2}}, \tag{7}$$

where k_{B} is the Boltzmann constant, T the absolute temperature, e the electron charge, $\Delta\nu$ the source spectral bandwidth, R the detector load resistance, η the detector responsivity, P the power of the detector, L the optical fiber coil length, A the fiber loss, and A_{C} includes other optical circuit losses. The model can be made to predict degradation of fiber optic gyro random walk coefficient based on fiber optic radiation attenuation curve.

To verify the RIA of fibers and the effects of all color centers on RWC and scale factor error of IFOGs, an experimental IFOG with sensing coils of F4, F5, and F6 is tested. The parameters of the IFOG and its physical quantities are shown in Table 7.

Table 7. Typical design parameters of experimental IFOG.

Parameter	Value	Parameter	Value
A_{C}/dB	18	D/mm	50
η/(A/W)	0.92	P/μW	180
$\Delta\nu$/Hz	6×10^{12}	λ/nm	1302
L/m	460	R/kΩ	800

Table 8 gives the calculated and tested results of the RWC as well as the scale factor error in the IFOG, and the contributions of all color centers are indicated. As can be seen in the table, both of the calculated and tested results are coincident. The RWC and the scale factor in the IFOG by using the P-doped fiber coil are more greatly affected than those by the Ge-doped and PSC fibers.

Table 8. Results of the effects of RIA spectra on the experimental IFOG at 1300 nm.

	Fibers	Contribution	Calculated RWC variation/((°)/h$^{-0.5}$)	Tested RWC variation/((°)/h$^{-0.5}$)	Contribution	Calculated scale variation/ppm	Tested scale variation/ppm
F4	P1	91.09%	0.8481	0.8030	91.21%	3777	3591
	Ge-NBOHC	8.91%			8.79%		
	Ge(X)	0			0		
F5	Ge-STH	99.37%	0.004	0.0036	98.26%	700	643
	Ge-NBOHC	0.625%			1.73%		
	Ge(X)	0.005%			0.01%		
F6	PSC-STH	100%	0.002	0.0017	100%	354	327
	Si-NBOHC	0			0		

5. Conclusions

In this paper, the RIA spectra in P-doped, Ge-doped, and PSC fibers with the radiation dose of 100 Gy and 1000 Gy ranging from 1100 nm to 1600 nm are measured. According to the Gaussian model, the RIA spectra of P-doped fibers are decomposed into P1, Ge-NBOHC, and Ge(X) color centers. The RIA spectra of Ge-doped fibers depend strongly on Ge-STH, Ge-NBOHC, and Ge(X) color centers, and the RIA spectra of PSC fibers are decomposed into STH and Si-NBOHC color centers. The relationship between color centers' absorption intensity and radiation dose is studied quantitatively and conforms to a power-law model, which is helpful in decomposing the spectrum into Gaussian functions with dynamic radiation dose. The effects of all color centers on the RIA and MWS in PMFs are investigated respectively. For the fibers and the tested IFOG, the P1 color centers account for a significant proportion in RWC variations and the scale factor variations in P-doped fibers, and almost all the total RWC and the scale factor variations are attributed to the STH band for Ge-doped and PSC fibers. Moreover, the RWC and the scale factor error of the IFOGs at 1300 nm are simulated based on color centers' absorption and also tested. The calculated and tested results of the RWC as well as the scale factor error in the IFOG are accordant with each other. Further studies should be conducted to investigate the cross effect of radiation and temperature on the RIA spectrum in space.

References

[1] Jin J, Tian H T, Pan X and Song N F 2010 *Chin. Phys. B* **19** 030701

[2] Lefevre H C 2014 *The Fiber-Optic Gyroscope*, 3rd edn. (London: Artech House) pp. 15–41

[3] Yang Y H, Suo X X and Yang W 2014 *Chin. Phys. B* **23** 094213

[4] Berghmans F, Brichard B and Fernandez A F, Gusarov A, Uffelen M V and Girard S 2006 *Proceeding of Optical Waveguide Sensing and Imaging* p. 127

[5] Jin J, Wang X Q, Song N F and Zhang C X 2010 *Sci. China- Tech. Sci.* **11** 3056

[6] Friebele E J, Askins C G, Miller G A, Peele J R and Wasserman L R 2004 *Proc. SPIE* **5554** 120

[7] Boucher R H, Woodward W F, Shima T S, Asman D J, Killian K M, Legrand J and Goellner G J 1996 *Opt. Eng.* **35** 955

[8] Williams G M and Friebele E J 1998 *IEEE Trans. Nucl. Sci.* **45** 1531

[9] Solé J G, Bausa L E, and Jaque D 2005 *An Introduction to the Optical Spectroscopy of Inorganic Solids* (John Wiley & Sons Ltd)

[10] Fang R C 2001 *Solid state spectroscopy* (Hefei: Press of China University of Science and Technology) p. 126 (in Chinese)

[11] Henderson B and Imbusch G F 1989 *Optical spectroscopy of inorganic solids* (New York: Clarendon Press of Oxford University) p. 192

[12] Griscom D L, Friebele E J, Long K J and Fleming J W 1983 *Appl. Phys.* **7** 3743

[13] Regnier E, Flammer I, Girard S, Gooijer F, Achten F and Kuyt G 2007 *IEEE Trans. Nucl. Sci.* **4** 1115

[14] Giacomazzi L, Martin-Samos L, Boukenter A, Querdane Y, Girard S and Richard N 2015 *Opt. Mater. Express* **5** 1054

[15] Friebele E J, Gingerich M E, Brambani L A, Harrington C C and Hickey S J 1990 *Proc. SPIE* **1314** 146

[16] Brichard B and Fernandez A F 1999 *Proc. RADECS Short Course* 137

[17] Griscom D L 1985 *SPIE Proc.* **541** 38

[18] Jin J, Liu J X, Wang X Q, Guo J H and Song N F 2013 *Lightwave Technol.* **6** 839

[19] Girard S, Ouerdane Y, Origlio G, Marcandella C and Boukenter A 2008 *IEEE Trans. Nucl. Sci.* **6** 3473

[20] Griscom D L, Friebele E J, Long K J and Fleming J W 1983 *Appl. Phys.* **7** 3743

[21] Wang X Q, Zhang C X and Jin J 2011 *Infrared and Laser Engineering* **11** 2516

[22] Friebele E J, Gingerich M E and Griscom D L 1992 *Survivability of optical fibers in space. Optical Materials Reliability and Testin* (Bellingham) p. 177

[23] Lef'evre H C 1997 *Proc. SPIE* **1** A20